

ESTIMATION OF SITE EFFECT, ATTENUATION AND SOURCE PARAMETERS IN WENCHUAN EARTHQUAKE BY SPECTRAL INVERSION METHOD

Yefei REN*
MEE11611

Supervisor: Hiroaki YAMANAKA **

ABSTRACT

With the demands of engineers and scientists, the spectral inversion method was used in present study to estimate simultaneously the site response, source parameters and S-wave attenuation (Q value) for the aftershocks of the Great 2008 Wenchuan Earthquake. In this regard, 602 recordings from 96 earthquakes associated at 28 stations were selected as a database.

After getting the inversion results, we compared the site response with the one calculated by the HVSR method and 1-D theory computation, and regressed the relationship between the site amplification and V_{s20} (the average uppermost-20m shear wave velocity) for different frequency bands. In addition, the inversed site response was used to identify the soil nonlinearity during strong motion. In present study, a new distance measure called the asperity distance D_{Aspt} was proposed for reasonably characterizing the source-to-site distance in large earthquake.

Furthermore, the term of S-wave attenuation, Q factor was obtained as a frequency-dependent function, $Q(f) = 100.6f^{1.1}$. The source parameters for each earthquake including the seismic moment (M_0), corner frequency (f_0), stress drop ($\Delta\sigma$) and source radius (r) were estimated by fitting a ω^{-2} model with the source spectrum from the inversion. A regression analysis yielded the valuable relationship between M_0 and f_0 , $\log M_0$ and M_s , and between M_w and M_s , respectively.

Keywords: Wenchuan Earthquake, Site effect, Source parameter, Q value, Spectral inversion.

1. INTRODUCTION, 2. METHODOLOGY, 3. DATABASE AND DATA PROCESSING

Due to page limitation, see my thesis paper.

4. RESULTS AND DISCUSSION

4.1. S wave attenuation

As one of the importance factor charactering ground motion attenuation, the quality factor $Q(f)$ value was obtained with dependent frequency. Considering the form of power function, it was fitted by $Q(f) = 100.6f^{1.1}$, with the correlation coefficient of 0.961. We compared our result with the one in Tangshan Area: $Q(f) = 67f^{1.1}$ (Zhang *et al.*, 2001). They used the same method with us to analysis the data from the aftershocks of 1976 Tangshan Earthquake. From Figure 1, we can find the Q value in

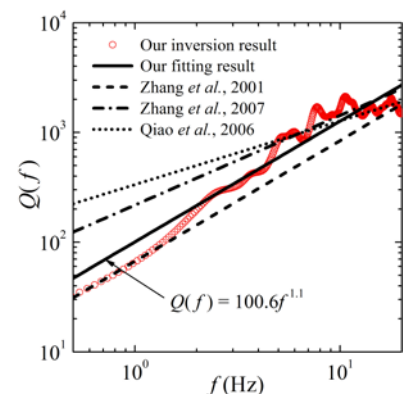


Figure 1. The quality factor $Q(f)$ from our spectral inversion

* Institute of Engineering Mechanics (IEM), CEA, Harbin, China.

** Professor, Tokyo Institute of Technology (TIT), Yokohama, Japan.

Sichuan Area is larger than in Tangshan Area but both of them have the same frequency dependence (same power value). That means the attenuation of S wave of Sichuan Area is lower than Tangshan Area that seems disagreeing with the accepted principle that the ground motion attenuation of the Western China is faster than the Eastern China. But it should be noted that the hypocenter distance of the data used by Zhang *et al.* (2001) is much closer (less than 50km) than this study that means the seismic wave propagate in the shallower crust. This is the most likely reason to explain why they got the lower Q value.

Furthermore, we compared our result with other studies which also focused on the Sichuan Area where the Wenchuan Earthquake occurred and affected. They are $Q(f) = 217.8f^{0.816}$ by Zhang *et al.* (2007) and $Q(f) = 334.4f^{0.581}$ by Qiao *et al.* (2006). As Figure 1 shows, the Q values of them are both larger than ours. As we above explained, the possible reason is that both of them used the data with farther hypocenter distance (10-400km) than our study that means the seismic wave propagate in the deeper crust.

4.2. Site effect

4.2.1 Site response analysis

The site response of 28 selected strong motion stations was achieved expectedly by the separation of source, path, and site effect. Meanwhile we calculated the site response by using 1-D theoretical computation and compared both of them with the results by HVSR method (Wen *et al.*, 2011). Figure 2 shows the results of the station 51GYZ. It should be noted that because we considered the free surface amplification that means the site response represents $2E_0/E$, we multiplied 2 of site amplification by HVSR method. There has a good agreement between the results from spectral inversion method and HVSR method in some stations, such as 51CXQ, 51GYQ, 51GYS, 51QLY and 62WIX. For most of stations, the site amplification of HVSR method is lower than the spectral inversion method, but the same predominant frequency.

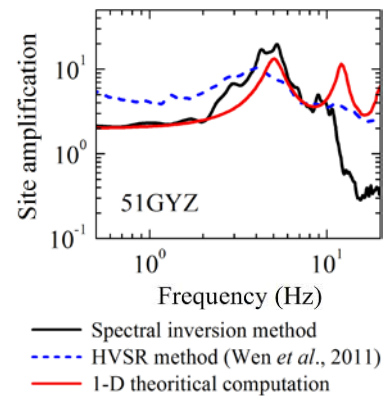


Figure 2. Site response of the station 51GYZ calculated by three methods

4.2.2 Predominant frequency and site amplification

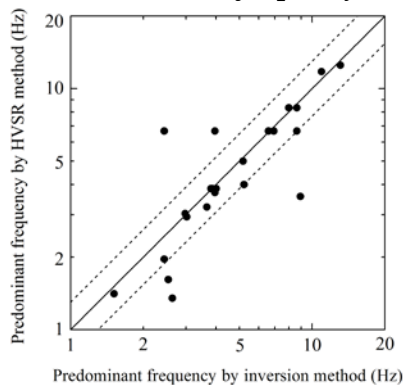


Figure 3. Comparison of the predominant frequency calculated by spectral inversion method and HVSR method

We compared the predominant frequency and average site amplification calculated by spectral inversion method and HVSR method (Wen *et al.*, 2011). As Figure 3 shows, the predominant frequency from two methods has a good agreement within 30% deviation. Another agreement is that there are two predominant frequencies for station 51LXS and 51WUD calculated by both methods with close values. But the average site amplification from HVSR method is lower than the spectral inversion method for frequency band 1.0-5.0Hz, 5.0-10.0Hz and 1.0-10.0Hz, as Figure 4 shows. For the frequency 0.5-1.0Hz band, it seems an agreement between them. The reason is the site response for this frequency band is slight even no amplification for some stations, almost equals to 2. Therefore, it can be concluded that the HVSR method can correctly evaluate the site predominant frequency but underestimate the site amplification. Such conclusion also has been made by some other previous studies.

4.2.3 Relation between site amplification and V_{s20}

There is available 20m borehole data for some stations. So we calculated the average shear wave velocity of upper 20m V_{s20} and the average site amplification for 0.5-10.0Hz, 1.0-5.0Hz, 5.0-10.0Hz and 1.0-10.0Hz frequency bands. We plotted the average site amplification versus V_{s20} in logarithmic

scale and found there has some relationship between them for each frequency band except 0.5-10.Hz, as Figure 5 shows. As we mentioned in above section, for 0.5-10.Hz frequency band, the site response is slight even no amplification for some stations. Because most of our used stations locate at tall-mountain area, the shallow surface soil layers only induce the high-frequency amplification.

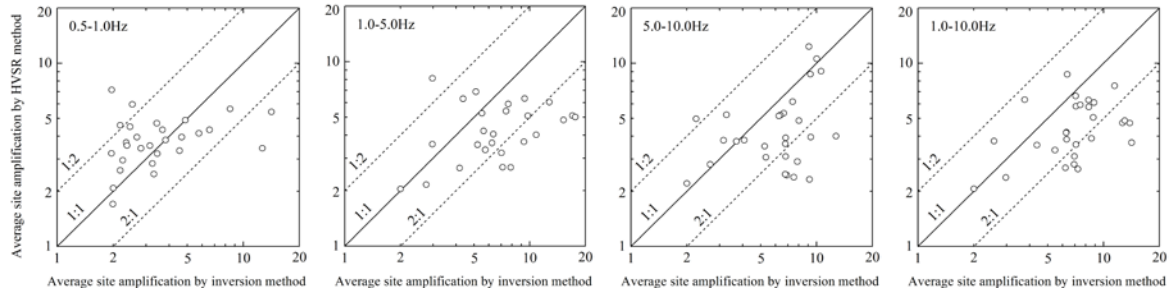


Figure 4. Comparison of the average site amplification calculated by spectral inversion method and HVSR method for each frequency band

We took a linear fitting in logarithmic scale and got the functions of site amplification as Vs20 for each frequency band, as seen in Figure 5. The results show it has a low correlation for 0.5-10.Hz band, but high correlation for other frequency bands.

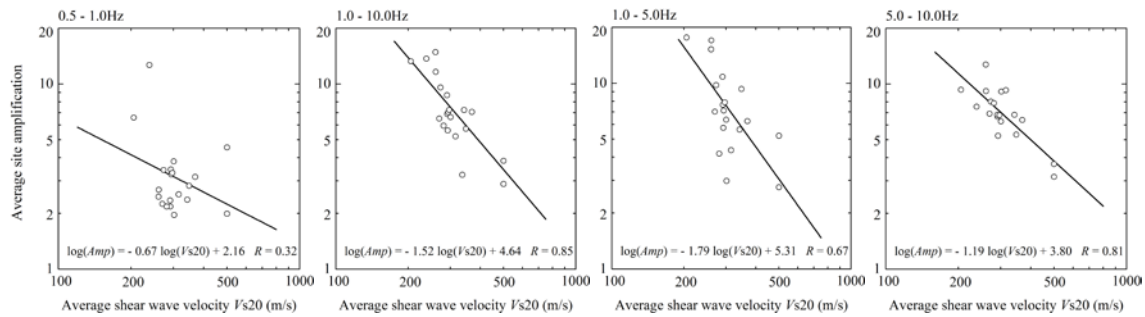


Figure 5. Average site amplification for 0.5-10.Hz, 1.0-10.0Hz, 1.0-5.0Hz and 5.0-10.0Hz frequency bands as a function of Vs20

4.2.4 Soil nonlinearity identification for aftershocks

For analyzing soil nonlinearity, we would compare the site amplification during strong motion and weak motion. For the weak motion, we already obtained the site amplification of each site by using spectral inversion method. Also we already obtained the path effect by means of frequency-dependent Q value, and the source spectrum as well. So the Eq. (3) of my thesis can be transformed into Eq. (14).

As we set the criteria to build the database in section 3, the definition of weak motion is that the average PGA of two horizontal components is below 100gal, on the contrary the strong motion is above 100gal. Therefore, we calculated the site effect by using Eq. (14) of my thesis for those recordings with $PGA > 100gal$.

Figure 6 shows for the station 51SFB it was identified there has a clear evidence of soil nonlinearity in the earthquake EQ080512144315 and EQ080512150134 that site amplification shifts towards the lower frequency during the strong motion than the weak motion, namely lower predominant frequency and deamplification in the high frequency part.

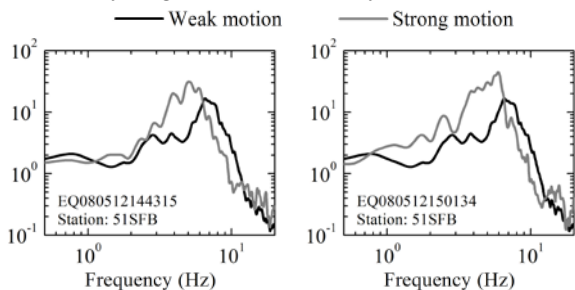


Figure 6. The obvious evidence presenting soil nonlinearity for station 51SFB

4.2.5 Soil nonlinearity identification for main shock

Among 28 stations of our database, only 51GYQ didn't capture the recording in the main shock because of the instrument malfunction. We added other 27 recordings into our database to take the spectral inversion again on the basis of the assumption that these recordings were obtained from another 26 stations except the reference station 62WIX. Then we can get another site response for each station after the spectral inversion. To compare them with previous result during weak motion we can identify the existence of soil nonlinearity in the main shock.

There has a basic assumption of earthquake point source for spectral inversion method. However, for the great Wenchuan Earthquake, the fault rupture process took long time and far distance. The point source assumption is not suitable for such large earthquake that means it should be took care of the distance R_{ij} . In this study, we proposed to use a new source-to-site distance measure called asperity distance D_{Aspt} by the following equation:

$$\ln D_{Aspt} = \frac{1}{A_{\Sigma}} \int_{\Sigma} \ln D(x, \xi) ds \quad (1)$$

where, $D(x, \xi)$ means the distance from the station x to a point ξ on the asperity region Σ , A is the total area of asperity. In fact D_{Aspt} represents a mean distance from the station to asperity. For the slip model of Wenchuan Earthquake, here we used the inversion result of finite fault model from USGS. According to the definition of asperity area by Somerville *et al.* (1999), we identified two asperities for Wenchuan Earthquake as shown in figure 7 and calculated the D_{Aspt} by Eq. (1). Also we calculated another three kinds of source-to-site distance measures which were widely used for ground motion attenuation analysis. There are the rupture distance (D_{Rup} , the shortest distance from the station to the rupture surface), Joyner-Boore distance (D_{JB} , the shortest horizontal distance to the vertical projection of the rupture) and hypocentral distance D_{Hyp} .

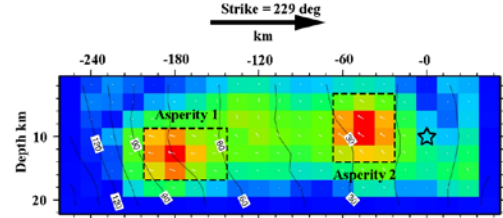


Figure 7. Two asperities were identified for Wenchuan Earthquake. Fault slip model is derived from USGS.

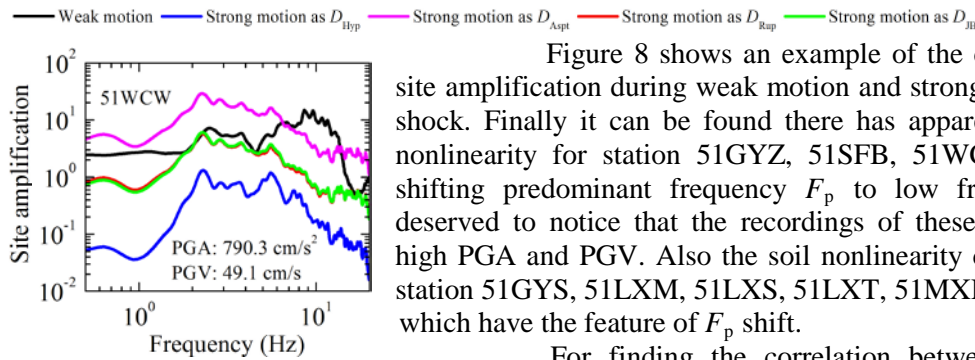


Figure 8. The example of the comparison between site amplification during weak motion and strong motion in the main shock of Wenchuan Earthquake

of them. Figure 9 shows this ratio versus the mean PGA and PGV of two horizontal components separately. It shows when the $PGA > 300 \text{ cm/s}^2$ or $PGV > 20 \text{ cm/s}$, the F_p will become much smaller for strong motion than for weak motion, namely the soil nonlinearity will significantly happen. And if

Figure 8 shows an example of the comparison between site amplification during weak motion and strong motion in the main shock. Finally it can be found there has apparent evidence of soil nonlinearity for station 51GYZ, 51SFB, 51WCW as significantly shifting predominant frequency F_p to low frequency part. It is deserved to notice that the recordings of these three stations have high PGA and PGV. Also the soil nonlinearity can be identified for station 51GYS, 51LXM, 51LXS, 51LXT, 51MXD, 51MXN, 62WUD which have the feature of F_p shift.

For finding the correlation between the nonlinearity level and ground motion level, we picked up the F_p for each station during weak motion and strong motion respectively and took the ratio

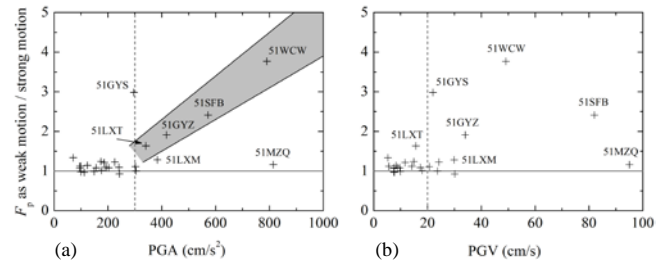


Figure 9. The predominant frequency F_p as weak motion over strong motion versus PGA and PGV

we see the shaded area of Figure 9, it can be found that the nonlinearity level will become larger when PGA value becomes larger.

4.3. Source parameters estimation

In present study, we proposed to use grid search technique to find the appreciate source parameters for each earthquake. We divided a range $M_s(M_1)-0.5 \leq M_w \leq M_s(M_1)+0.5$, $2-0.3 \leq \gamma_i \leq 2+0.3$ as a convenient preconception for high frequency spectral fall-off range by supposing ω^2 model, and $0.1 \leq f_{0i} \leq 5.0\text{Hz}$ considering the magnitude range of $3.7 \leq M_s(M_1) \leq 6.5$ to estimate an optimal set of M_w , γ_i and f_{0i} for the best fitting source spectrum by using Eq. (2):

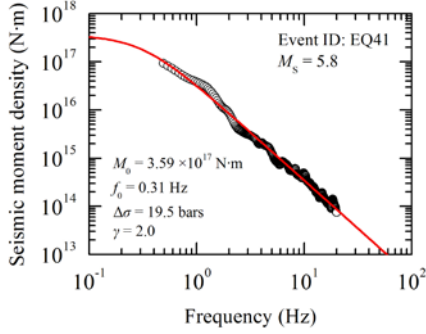


Figure 10. The inversed (circles) and the best-fitting (red line) seismic moment density for an exemplified event

$$\dot{M}_{0i}(f) = \frac{M_{0i}}{1 + \left(\frac{f}{f_{0i}}\right)^{\gamma_i}} \quad (2)$$

when the defined root mean square error between our inversed seismic moment density and its empirical value by Eq. (3) is smallest as follows,

$$R.M.S_i(M_w, \gamma, f_0) = \sqrt{\frac{\sum_j^N [\log(\dot{M}_{0i}^{Inv}(f_j)) - \log(\dot{M}_{0i}^{Emp}(f_j))]^2}{N}} \quad (3)$$

where, $\dot{M}_{0i}^{Inv}(f_j)$, $\dot{M}_{0i}^{Emp}(f_j)$ are the inversed and empirical seismic moment density at j th frequency for i th earthquake, respectively. N means the number of available frequency points.

Figure 10 shows a demonstration of the best-fitting seismic moment density for one event. The relationship between M_0 and f_0 was linearly fitted in logarithmic scale as follows:

$$\log(M_0) = (22.77 \pm 0.04) - (2.37 \pm 0.08) \log(f_0) \quad (4)$$

Considering the assumption of $M_0 \propto f_0^{-3}$ by Aki (1967), which corresponds to constant stress drop, the regression of the data yielded

$$\log(M_0) = (22.83 \pm 0.42) - (3) \log(f_0) \quad (5)$$

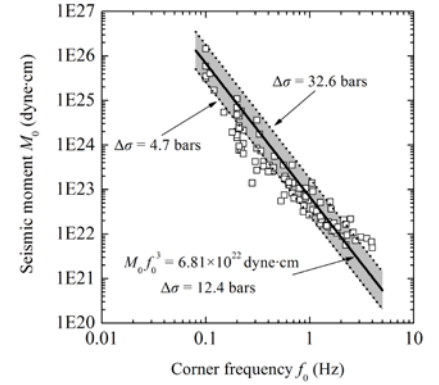


Figure 11. Seismic moment versus corner frequency obtained from inversion analysis. The shaded area of this figure means the area of one standard deviation of the mean value. Eq. (5) also can be written as $M_0 f_0^3 = 6.76 \times 10^{22}$ dyne·cm corresponding to a constant stress drop 12.4 bars.

Figure 11. Seismic moment versus corner frequency obtained from inversion analysis

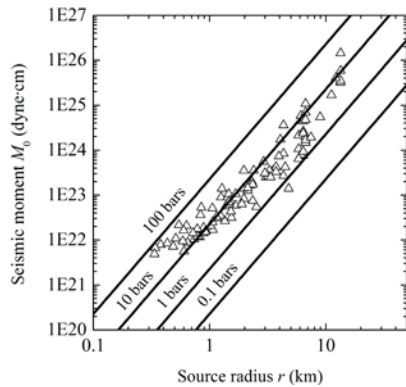


Figure 12. Seismic moment versus source radius for each event

According to the ω^2 model of, the source radius (r_i) and stress drop ($\Delta\sigma_i$) for i th event can be calculated by Eq.(28) and Eq.(29) of my thesis.

Figure 12 shows the seismic moment versus source radius for 96 aftershocks of the Wenchuan Earthquake. It can be found that expect for one event, the stress drop varies between 1 bars to 100bars. Figure 13 shows the regression analysis between $\log M_0$ and M_s , M_w and M_s . It yielded the relationship:

$$\log M_0 = (1.475 \pm 0.06) M_s + (16.09 \pm 0.31) \quad (6)$$

$$M_w = (0.917 \pm 0.04) M_s + (0.33 \pm 0.19) \quad (7)$$

Then we compared Eq. (6) with the accepted relationship between $\log M_0$ and M_w : $\log M_0 = 1.5 M_w + 16.05$. The result shows that two relationships are in close agreement with each other, in other words, M_w almost can be replaced by M_s in Wenchuan area approximately that is also deduced from Eq. (7).

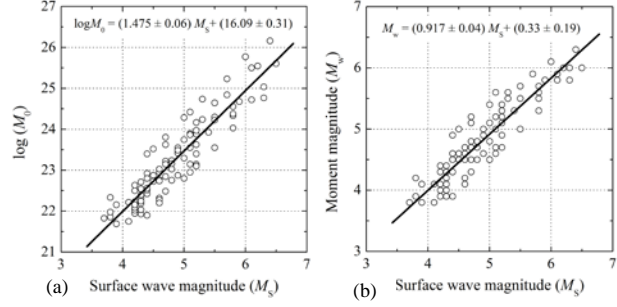


Figure 13. The regression between $\log M_0$ and M_s (a), M_w and M_s (b)

5. CONCLUSIONS

Using spectral inversion method, the source spectrum, site response and attenuation (representation of Q factor) of S wave were separated for the aftershocks of the 2008 Great Wenchuan Earthquake. By analyzing the inversion results, we concluded that:

(1) The site response of 28 strong motion stations was evaluated by inversion method, HVSR method and 1-D theoretical computation. (2) The deficiency of HVSR method was also found in present study through comparing with the inversion results that it can reasonably estimate the site predominant frequency but underestimate the site amplification. (3) The site amplification in Wenchuan Area was evaluated as a function of V_{s20} (the average uppermost-20m shear wave velocity) for 1.0-5.0Hz, 5.0-10.0Hz and 1.0-10.0Hz frequency bands, respectively. (4) It was identified the soil nonlinearity in the aftershocks of Wenchuan Earthquake was existed only at the station coded 51SFB (5) A new distance measure called the asperity distance D_{Aspt} was proposed for reasonably characterizing the source-to-site distance in large earthquake, like Wenchuan Earthquake of present study. (6) The comparison of site response between main shock and aftershocks shows ten stations induced soil nonlinearity during main shock. It was found that a threshold $PGA > 300 \text{ cm/s}^2$ or $PGV > 20 \text{ cm/s}$ was obviously existed for soil nonlinearity in Wenchuan Earthquake and the nonlinearity level was significantly dependent on the ground motion level corresponding to the PGA and PGV . (7) The quality factor Q in terms of S-wave attenuation was estimated by a frequency dependent function $Q(f) = 100.6f^{1.1}$ at the frequency band 0.5-20.0 Hz within the propagation distance range of 30-150 km. (8) The grid search technique was proposed in this study for determining the best appreciate source model for each earthquake. Then the source parameters including M_0 , f_0 , $\Delta\sigma$ and r were estimated finally. The regression analysis yielded a relationship between seismic moment and corner frequency $M_0 f_0^3 = 6.76 \times 10^{22} \text{ dyne}\cdot\text{cm}$ corresponding to a constant stress drop 12.4 bars, in the M_0 range of $10^{21} \leq M_0 \leq 10^{27} \text{ dyne}\cdot\text{cm}$. Moreover, the regression analysis also yielded two linear relationships between $\log M_0$ and M_s and between M_w and M_s which can be used for further research.

ACKNOWLEDGEMENT

I would like to express my sincere gratitude to my adviser Dr. T. Kashima for his helpful suggestions for choosing this topic and some comments of final review of this paper.

REFERENCES

- Aki, K., 1967, J. Geophys. Res., 72, 1217-1231.
 Qiao, H. Z., *et al.*, 2006, Seismol. Geomagn. Obs. Res., 27, 1-7 (In Chinese with English abstract).
 Somerville, P., *et al.*, 1999, Seismol. Res. Lett., 70, 59-80.
 Wen, R. Z., Ren, Y. F. and Shi, D. C., 2011, Earthquake Eng. Eng. Vibr., 10, 325-337.
 Zhang, W. B., Xie, L. L. and Guo, M. Z., 2001, China, Acta Seismol. Sin., 14, 642-653.
 Zhang, Y. J., *et al.*, 2007, J. Seismol. Res., 30, 43-48 (In Chinese with English abstract).